



## Effect of spin-orbit interaction on the band structures of *d*-band metals

Lalnunpuia, Aldrin Malsawmtluanga, Ricky L. Ralte and Z. Pachuau\*

*Department of Physics, Mizoram University, Aizawl 796004, India*

Received 29 April 2015 | Revised 15 May 2015 | Accepted 9 June 2015

### ABSTRACT

We present here the electronic structure calculations of *d*-band metals like W and Cr using a self-consistent, full-potential linearized augmented plane wave (FP-LAPW) method. We performed a scalar relativistic calculation without spin-orbit interaction (NSOI) and a fully relativistic with spin-orbit interaction (SOI) included in a second-variational treatment. We found close agreement between our calculations and the experimental results. The calculated Fermi energy for SOI and NSOI are same and almost equal to the experimental value. We found that the effect of spin-orbit interaction (relativistic effect) increases with the atomic number.

**Key words:** Energy band structure; density of states; spin-orbit interaction; FP-LAPW.

**PACS No:** 71.15; 71.20; 71.70

### INTRODUCTION

Spin-orbit interaction (SOI) is a well known factor for splitting of degenerate electron energy levels in atoms, molecules and solids. It has played in the past an important role in describing the band structure of semiconductors<sup>1,2</sup> and in explaining various splitting of surface states.<sup>3-6</sup> Its physical origin is relativistic and can be explained by the interaction of the magnetic momentum of the electron (spin) with the magnetic field viewed by this electron because of its move-

ment in the electrostatic field of the proton.

Relativistic effects become important in heavier elements, particularly in *5d* transition metals and actinides. They can substantially influence many characteristics (like densities of states and photoemission spectra) of such systems. Their interplay with the spin polarization affects the magnetic structure, values of magnetic moments and lead to a number of important effects such as magnetic anisotropies or magneto-optical phenomena.<sup>7,8</sup>

The electronic and optical properties of W using non-self-consistent, self-consistent, non-relativistic and scalar-relativistic electronic band structure calculations have been reported by a

Corresponding author: Pachuau  
 Phone: +91-9862770341  
 E-mail: [zpc21@yahoo.com](mailto:zpc21@yahoo.com)

number of authors.<sup>9-11</sup> Using naval research laboratory tight-binding (NRLTB) method<sup>12-14</sup> that includes the SOI, the effect on the equilibrium volume, band structure, and density of states in the  $5d$  series of the transition metals were presented.<sup>15</sup> Their results show that near  $E_F$ , the difference between SOI and non-SOI is small, which gives negligible changes to the Fermi surface and to the value of the density of states at  $E_F$ .

In the *bcc* Cr metal, because of its half-filled valence configuration  $3d^64s^1$ , it yields both a large magnetic moment and strong inter-atomic bonding which leads to magnetic frustration.<sup>14</sup> The results of a fully relativistic band-structure calculation using the relativistic-augmented plane-wave (RAPW) method<sup>15</sup> were very similar to the non-relativistic band structure.

In the present work, we report the full-potential linearized augmented plane wave method (FP-LAPW) calculations of equilibrium lattice constant, density of states and energy band structure of W and Cr. The aim of this work is to study the effect of SOI using WIEN2k code<sup>16</sup> that provides a scheme for the calculation of scalar relativistic and fully relativistic electronic structure.

## METHODS

The calculations were done using a mixed basis APW+*lo*/LAPW method.<sup>17</sup> The addition of the new local orbital (*lo*) gives the radial basis functions more variational flexibility. In the code, the basis set APW+*lo* is used inside the atomic spheres for the chemically important orbitals, which are difficult to converge, whereas the LAPW basis set is used for others. A gradient corrected Perdew-Berke-Ernzerhof (PBE) functional generalized gradient approximation (GGA) is used to describe the exchange and correlation effects.<sup>18-21</sup> As far as relativistic effects are concerned, core states are treated fully relativistically and two levels of treatments are implemented for valence states: (1) a scalar relativistic scheme (without SOI) that describes the

main contraction or expansion of various orbitals due to the mass-velocity correction and the Darwin *s*-shift<sup>20</sup> and (2) a fully relativistic scheme with SOI included in a second-variational treatment using the scalar-relativistic eigen-functions as basis.<sup>21</sup>

All calculations involved discretizing the first Brillouin zone and a cut-off of -9.0 (for tungsten) and -6.0 (for chromium) Ryd, were used to discriminate between core and valence (or semi-core) states. A constant muffin-tin (MT) radius ( $R_{MT}$ ) used are given in Table 1. The potential and charge density representations inside the MT spheres are expanded with  $l_{max}=10$ . The number of plane waves in the interstitial was

limited by the cutoff value of  $R_{MT}^{min} K_{max} = 7$  (that is the product of the smallest atomic sphere and the largest reciprocal lattice vector was 7), where  $K_{max}$  is the plane wave cut-off and  $R_{MT}$  is the smallest of all atomic sphere radii. The charge density was expanded with  $G_{max}=12$ . The self-consistent calculations are considered to be converged when the total energy of the system is stable within 0.0001 Ryd and a charge convergence criterion of 0.001  $e^-$ .

The volume optimization curves were obtained by calculating the total energy at different volumes around equilibrium and by fitting the calculated values to the Murnaghan's equation of state.<sup>22</sup> Then by using the volume corresponding to the lowest energy, we calculated the value of lattice constant for W and Cr. By using this value of the lattice constant, we calculated the band structures along symmetry lines in the Brillouin zone.

The experimental lattice constant  $a = 3.1652$

Table 1. Input parameters used for calculation of DOS and band structure.

Structure	Space Group	Lattice constant (Å)		$R_{MT}$ (Å)
		SOI	NSOI	
<i>bcc</i> Chromium	Im-3m (229)	2.8824	2.8824	2.2
<i>bcc</i> Tungsten	Im-3m (229)	3.1588	3.1588	2.0

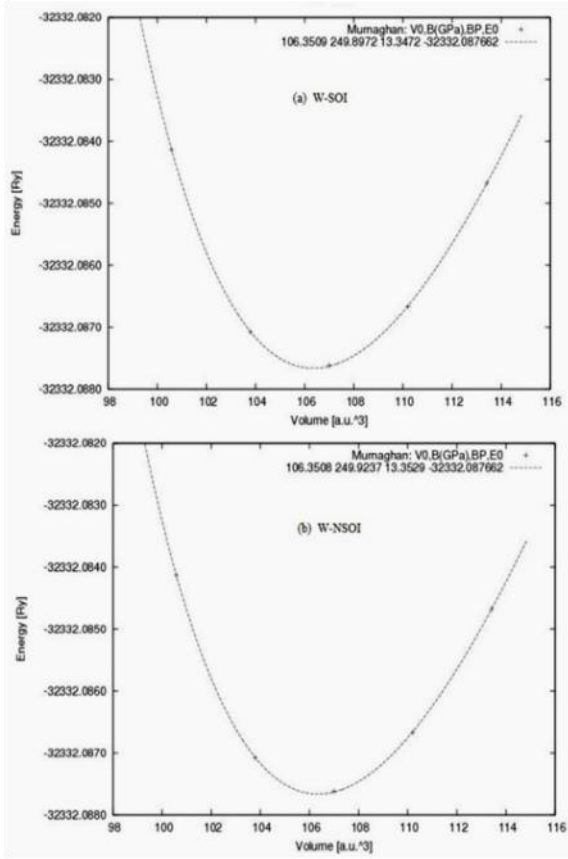


Figure 1. Total energy as a function of volume for W with SOI and without SOI (NSOI).

and  $2.8824 \text{ \AA}$  respectively were used<sup>23</sup> for body-centered-cubic (*bcc*) W and Cr. The other parameters used in the calculation are given in Table 1. The zero for the energy scale of the calculated DOS is always placed at the top of the valence band, i.e. the energy of highest occupied state. All states at negative energies are therefore occupied in the ground state, while all states positive energies are unoccupied.

## RESULTS AND DISCUSSION

### Tungsten (W)

The transition metal tungsten is *bcc*, with six valence electrons distributed among the  $5d$  and

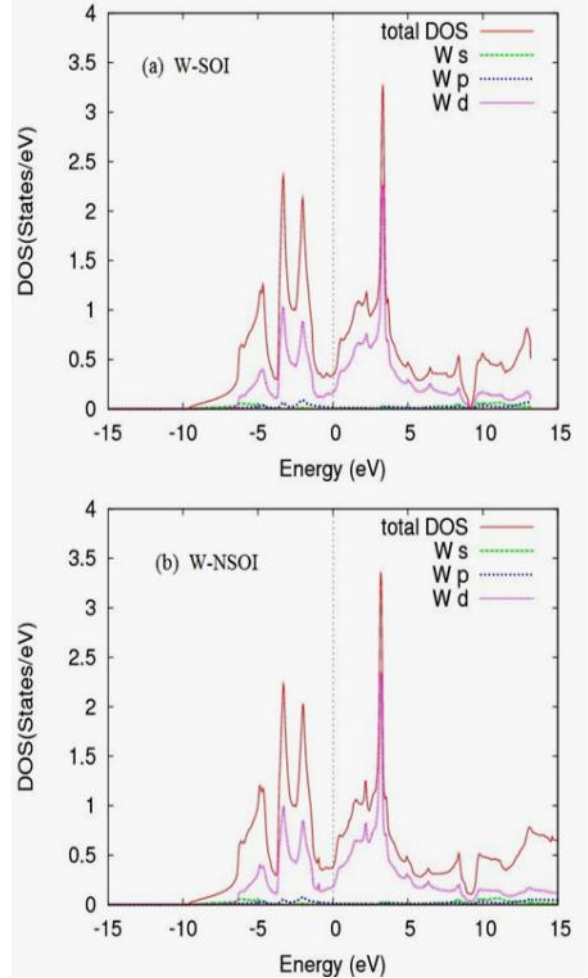


Figure 2. Density of states for W in the case of (a) SOI and (b) without SOI (NSOI).

$6sp$  orbitals. The variation of total energy as a function of volume is shown in Figure (1) for W, in the case of SOI and NSOI. The calculated the value of lattice constant of  $W a = 3.1588 \text{ \AA}$  (both for SOI and NSOI) is in agreement with the experimental value (Table 1).<sup>24</sup> From the calculated the band structure, the Fermi level  $E_F$  is close to the centre of the  $d$  bands as expected. Since the  $d$  states of  $W$  whose valence shell electronic configuration is  $5d^46s^2$ , it is approximately half-filled.

If we compare the band structure of  $W$  with SOI and without SOI (NSOI) at  $\Gamma$ , the state

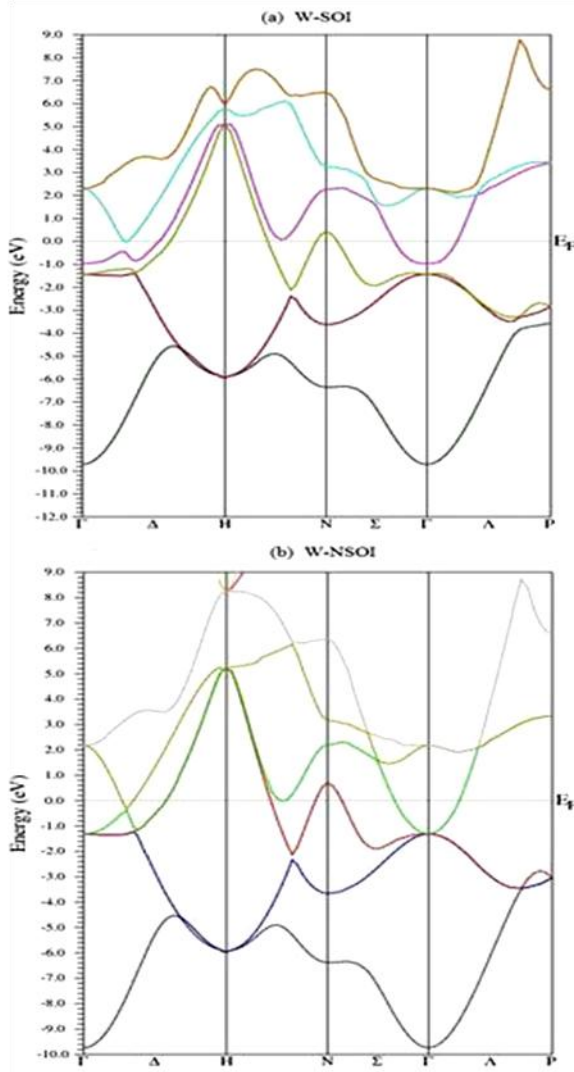
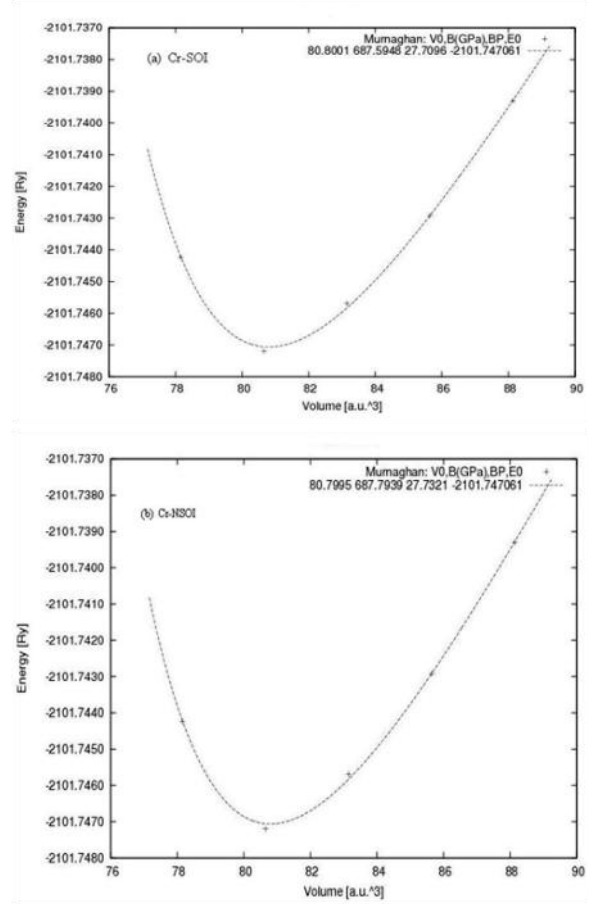


Figure 3. Energy band structure of W (a) with SOI and (b) without SOI (NSOI).

splits into a doubly degenerate and non-degenerate. Similarly, the triple degenerate state splits into a double degenerate and a non-degenerate. There is no splitting due to SOI along  $\Gamma$ -N direction. In the direction  $\Gamma$ -H near  $E_F$ , there is a change which may have an effect on the Fermi surface around  $\Gamma$ . In the scalar-relativistic band structure calculation (Figure 2b), three bands cross the Fermi level, one of which is doubly degenerate. The SOI lifts this



degeneracy and three bands appear with  $\Delta_7$  sym-

Figure 4. Total energy as a function of volume for Cr with SOI and without SOI (NSOI).

metry. Their mutual repulsion creates a small energy gap at the Fermi energy as in Figure 3(a).

From Figures (1) and (2), which give variation of total energy as a function of volume and the density of states of W for SOI and NSOI, the difference between SOI and NSOI is very small. The reason is that in the *bcc* structure away from the centre of the Brillouin zone, there are not as many splitting due to SOI as in the case of the *fcc* structure.<sup>12</sup>

The calculated Fermi energy for both SOI and NSOI are same (17.49 eV) and are larger than experimental data<sup>24</sup> of 11.3 eV. SOI split-

Table 2. Calculated SO splitting energy along three high-symmetry k points ( $\Gamma$ , H, and P) and d-band widths for W and Cr. All energies are measured with respect to the Fermi energy.

Metal	SOI splitting energy (eV)			
	$\Gamma$	H	P	Others
Cr	-	-	-	-
W	0.47	0.66	0.73	0.45 <sup>b</sup>
Width of <i>d</i> -band (eV)				
Metal	SOI	NSOI	Others	
Cr	6.5	6.5	~7 <sup>a</sup> , 7.77 <sup>c</sup>	
W	11.9	11.15	12.26 <sup>d</sup>	

<sup>a</sup>Ref-29; <sup>b</sup>Ref-28; <sup>c</sup>Ref-30; <sup>d</sup>Ref-31

ting energy (eV) along the symmetry line for W (shown in Table 2) in each case for the three high-symmetry k points  $\Gamma$ , H, and P are 0.47, 0.66, and 0.73 eV respectively. The SOI splitting at  $\Gamma$  point i.e. 0.47 eV is almost the same as compared with experimental value.<sup>25</sup>

On comparison to the results obtained using other methods like the linearized augmented plane wave method<sup>26</sup>, the relativistic-augmented plane-wave method<sup>9,27</sup>, using naval research laboratory tight-binding (NRLTB) method<sup>11</sup> and also the full-potential linearized augmented-plane wave (FP-LAPW) method,<sup>16</sup> our result showed agreement with the earlier result of other workers.

### Chromium

Plot of total energy as a function of volume for Cr in the case of SOI and NSOI are given in Figure (4). The lattice constants obtained by choosing the volume corresponding to the lowest value of the energy are same for both SOI and NSOI i.e. 2.8824 Å which is very close to the experimental value<sup>24</sup> of 2.882 Å. These theoretical values of the lattice constants obtained are then used in the band structure calculations.

The band structures of Cr along the high symmetry points in the Brillouin zone are

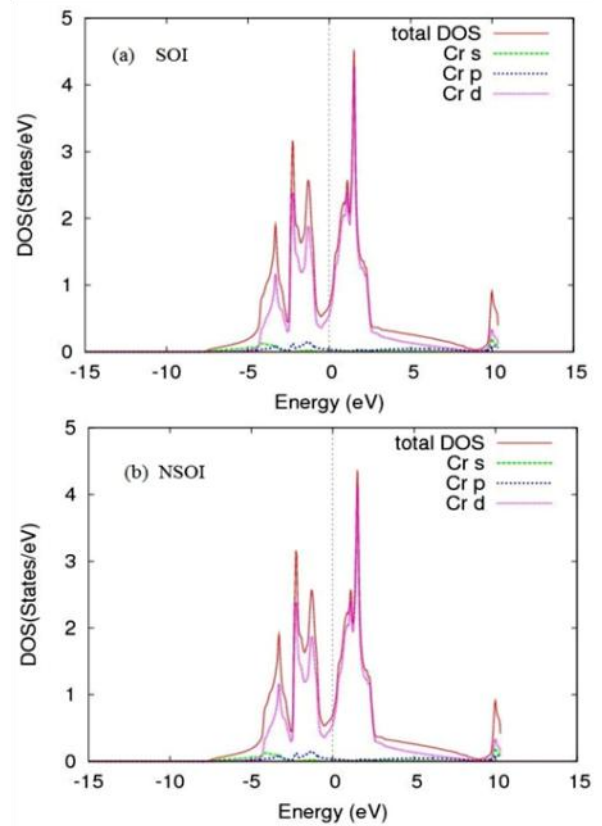


Figure 5. Density of states for Cr in the case of (a) SOI and (b) without SOI (NSOI).

shown in Figure (6). Fermi level  $E_F$  is close to the centre of the *d* bands as can be seen from the valence shell electronic configuration  $3d^4 4s^1$ , which is half-filled. The calculated value of the Fermi energy of Cr i.e. 10.52 eV, is set as zero in the band structure plot. If we compare the band structure of Cr including SOI and NSOI, we find no significant effect in the case of SOI. Also the calculated Fermi energy for SOI and NSOI are same and are almost the same as the experimental value  $E_F=10.6$  eV.<sup>24</sup>

From Figures (4) and (5), which give the variation of total energy as a function of volume and density of states (DOS) for Cr with SOI and without SOI (NSOI), the difference between SOI and NSOI is very small. The width of *d*-band in the case when SOI is included is found

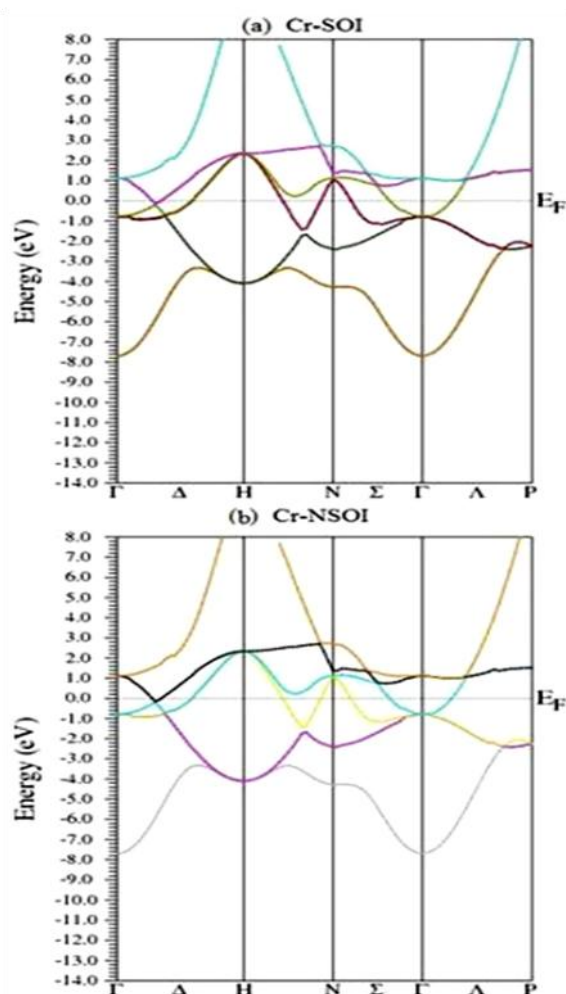


Figure 6. Energy band structure of Cr (a) with SOI and (b) without SOI (NSOI).

out to be 6.5 eV which is the same as for NSOI, and is relatively small with compared to the result of others.<sup>28,29</sup> The calculated results for DOS and band structure show agreement to the earlier calculated results.<sup>30</sup>

## CONCLUSION

We found that in case of *d*-band metals discussed above, our calculated results for DOS and band structure showed agreement to the calculated results of other workers<sup>28-30</sup>. However,

in the case of band structure of Cr, the lowering of the spectrum which is a manifestation of the mass-velocity and Darwin effects arising in the relativistic theory cannot be found although the curves are scalar-relativistic and relativistic including SOI respectively. Also the influence of the SOI in anti-ferromagnetic Cr is seen to be insignificant whereas in W, SOI influence is more pronounced showing that the effect of spin-orbit interaction (relativistic effect) increases with the atomic number.

## ACKNOWLEDGEMENT

LNP gratefully acknowledges a research grant from the University Grants Commission-North Eastern Regional Office (UGC-NERO), Guwahati, India.

## REFERENCES

1. Kane EO (1956). Energy band structure in p-type germanium and silicon. *J Phys Chem Solids*, **1**, 82–99.
2. Braunstein R & Kane EO (1962). The valence band structure of the III–V compounds. *J Phys Chem Solids*, **23**, 1423–1431.
3. LaShell S, McDougall BA & Jensen E (1996). Spin splitting of an Au (111) surface state band observed with angle resolved photoelectron spectroscopy. *Phys Rev Lett*, **77**, 3419–3422.
4. Petersen L & Hedegard P (2000). A simple tight-binding model of spin–orbit splitting of sp-derived surface states. *Surf Sci*, **459**, 49–56.
5. Nicolay G, Reinert F, Hüfner S & Blaha P (2002). Spin-orbit splitting of the L-gap surface state on Au (111) and Ag (111). *Phys Rev B*, **65**, 033407–4
6. Henk J, Ernst A & Bruno P (2003). Spin polarization of the L-gap surface states on Au (111). *Phys Rev B*, **68**, 165416–9.
7. Rotenberg E, Chung JW & Kevan SD (1999). Spin-orbit coupling induced surface band splitting in Li/W (110) and Li/Mo (110). *Phys Rev Lett*, **82**, 4066–4069.
8. Christensen NE & Feuerbacher B (1974). Volume and surface photoemission from tungsten. I. Calculation of band structure and emission spectra. *Phys Rev B*, **10**, 2349–2372.
9. Jansen HJF & Freeman AJ (1984). Total energy full-potential linearized augmented-plane-wave method for

- bulk solids: Electronic and structural properties of tungsten. *Phys Rev B*, **30**, 561–569.
10. Lee MJG & Ibrahim ZA (2004). Electronic structure of tungsten surfaces and total energy distributions of the field emission current. *Phys Rev B*, **70**, 1254301–1254309.
  11. Papaconstantopoulos DA & Mehl MJ (2005). Tight binding method in electronic structures. In: *Encyclopedia of Solid State Physics*, Elsevier, Amsterdam, pp. 194–206.
  12. Lach-Hab MM & Papaconstantopoulos DA (2008). The effect of spin-orbit coupling on the band structure of 5d metals. *Phil Mag*, **88**, 18–20, 2799–2805.
  13. Cheng H & Wang LS (1996). Dimer growth, structural transition and antiferromagnetic ordering of small chromium clusters. *Phys Rev Lett*, **77**, 51–54.
  14. Kohl C & Bertsch GF (1999). Noncollinear magnetic ordering in small chromium clusters. *Phys Rev B*, **60**, 4205–4211.
  15. Loucks TL (1967). *Augmented Plane Wave Method*. Benjamin, New York
  16. Blaha P, Schwarz K, Madsen GKH, Kvasnicka D & Luitz J (2008). *WIEN2k*, An Augmented Plane Wave + Local Orbitals Program for Calculating Crystal Properties (Karlheinz Schwarz, Techn. Universitat Wien, Austria).
  17. Singh DJ (1994). *Plane waves, Pseudo potentials, and LAPW Method*. Kluwer Academic Publishers, Boston, Dordrecht, London and references therein.
  18. Perdew JP, Burke S, Ernzerhof M (1996). Generalized gradient approximation made simple. *Phys Rev Lett*, **77**, 3865–3868.
  19. Perdew JP & Wang Y (1992). Accurate and simple analytic representation of the electron-gas correlation energy. *Phys Rev B*, **45**, 13244–13249.
  20. Koelling DD & Harmon BN (1977). A technique for relativistic spin-polarized calculations. *J Phys C: Sol Stat Phys*, **10**, 3107–3114.
  21. Novak P (1997). See \$WIENROOT/SRC/novak\_lecture\_on\_spinorbit.ps (WIEN2k 04)
  22. Murnaghan FD (1944). The compressibility of media under extreme pressures. *Proc Natl Acad Sci USA*, 244–247.
  23. Brandes EA & Brook GB (ed) (1992). *Smithells Metals Reference Book*. The Bath Press, Bath, Great Britain
  24. Irkhin V Yu & Irkhin Yu P (2000). Electronic structure, correlation effects and physical properties of *d*- and *f*-transition metals and their compounds. [*arXiv:cond-mat/9812072v2*, 18 May 2000]
  25. Herman F & Skillman S (1963). *Atomic Structure Calculations*. Prentice-Hall, Englewood Cliffs, NY
  26. Wei SH & Krakauer H (1985). Linearized augmented-plane-wave calculation of the electronic structure and total energy of tungsten. *Phys Rev B*, **32**, 7792–7797.
  27. Ahuja BL, Rathor A, Sharma V, Sharma Y, Jani AR & Sharma B (2008). Electronic Structure and Compton Profiles of Tungsten. *Z Naturforsch*, **63A**, 703–711.
  28. Pieve F Da & Kruger P (2013). First-principles calculations of spin and angle-resolved resonant photoemission spectra of Cr(110) surfaces at the *2p-3d* resonance. (*arXiv:1302.7160v1 [cond-mat.str-el]*, 28 Feb 2013).
  29. Sigalas M, Papaconstantopoulos DA & Bacalis NC (1992). Total energy and band structure of the *3d*, *4d* and *5d* metals. *Phys Rev B*, **45**, 5777–5783.
  30. Moruzzi VL & Marcus PM (1993). In: *Handbook of Magnetic Materials*. (Ed.) Buschow KHJ, North Holland, Amsterdam. Vol. 7.